Available online at www.sciencedirect.com

ScienceDirect

www.elsevier.com/locate/jes

JES JOURNAL OF ENVIRONMENTAL SCIENCES

www.jesc.ac.cn

Analysis of amino acid enantiomers in ambient aerosols: Effects and removal of coexistent aerosol matrix

Ying Li[1], *Xiaoying Li*[1], *Libin Wu*[2], *Luhan Shi*[1], *Shan Wang*[1,3], *Pingqing Fu*[2], *Yingyi Zhang*[1,*], *Senchao Lai*[1,*]

[1] *The Key Lab of Pollution Control and Ecosystem Restoration in Industry Clusters, Ministry of Education, School of Environment and Energy, South China University of Technology, Guangzhou 510006, China*
[2] *Institute of Surface-Earth System Science, School of Earth System Science, Tianjin University, Tianjin 300072, China*
[3] *now at Hong Kong University of Science and Technology, Hong Kong 00852, China*

ARTICLE INFO

Article history:
Received 26 October 2022
Revised 24 February 2023
Accepted 24 February 2023
Available online 5 March 2023

Keywords:
Amino acid enantiomers
Atmospheric aerosol
Organic carbon
Ammonia
Chiral ratio

ABSTRACT

Amino acids (AAs) including D- and L- enantiomers are a group of organic nitrogen species in ambient aerosol. Due to the low abundances of AAs (level of ng/m^3) and the matrix effects by coexistent components, it is challenging to quantify AA enantiomers in ambient aerosols especially under pollution conditions. In this study, we present an optimized method for analyzing AA enantiomers in atmospheric aerosol samples including a pretreatment process and the detection by high performance liquid chromatography coupled to a fluorescence detector (HPLC-FLD). Matrix effects caused by coexistent chemicals on AA enantiomers analysis in ambient aerosol samples were investigated especially for those collected in pollution episodes. The results revealed that the determination of AA enantiomers is significantly affected by the coexistent organic carbon (as a proxy of organic matter) and water-soluble ion of NH_4^+. To remove the matrix effects, we applied a pretreatment using the solid phase extraction column coupled with alkaline adjustment to sample extract. After pretreatment, 18 AAs including 6 pairs of D- and L-enantiomers (i.e., leucine, isoleucine, valine, alanine, serine, and aspartic acid) can be successfully separated and quantified in aerosol samples by HPLC-FLD. The recoveries are in the range of 67%-106%. This method was successfully applied to the urban aerosol samples from pollution and non-pollution periods for AA enantiomers determination. We suggest that the concentrations of D-AAs and the ratio of D-AA/L-AA are indicative of the contribution of bacterial sources and the influence of biomass burning.

Introduction

Amino acids (AAs) are ubiquitous organic nitrogen species in atmospheric aerosol particles involved in the global nitrogen cycle. They can act as cloud condensation nuclei to retain water at low relative humidity (Chan et al., 2005; Di Filippo et al., 2014; Szyrmer and Zawadzki, 1997). AAs can affect the input of organic nitrogen into marine ecosystems, the atmospheric radiation balance and the global water cycle (Scalabrin et al., 2012). Among the AAs, glycine (Gly) is a nonchiral compound while many AAs have two enantiomers (i.e., D- and L-form).

* Corresponding authors.
E-mails: zhyy@scut.edu.cn (Y. Zhang), sclai@scut.edu.cn (S. Lai).

https://doi.org/10.1016/j.jes.2023.02.048
1001-0742/

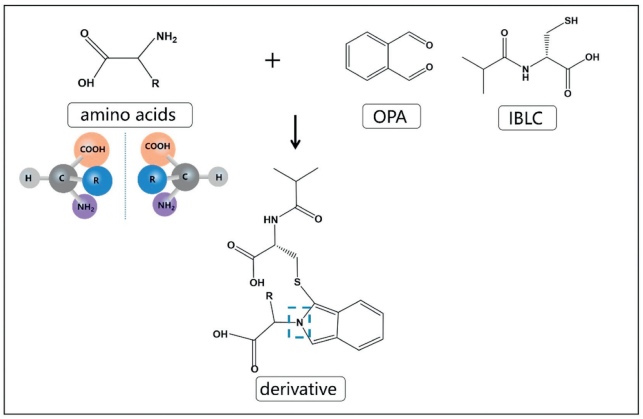

Fig. 1 – Molecular structure of amino acid enantiomers and amino acid derivation reaction. The blue box represents the group and sites of the reactions from which amino acids are derived.

The molecules of the AA enantiomer are mirror symmetric (Fig. 1). L-AAs are the most common enantiomers in nature because most organisms use only L-AAs for the biosynthesis of proteins and peptides. D-AAs are rarely found but mainly exist in the cell wall of bacteria (e.g. D-alanine (D-Ala), D-serine (D-Ser), D-glutamic acid (D-Glu) and D-aspartic acid (D-Asp) (Dittmar et al., 2001; McCarthy et al., 1998; Perez et al., 2003) and marine phytoplankton (e.g. D-leucine (D-Leu) and D-isoleucine (D-Ile) (Wedyan and Preston, 2008)). In a natural environment such as in ambient air, it takes a long time for L-AAs to convert to D-AAs. Therefore, the occurrence of D-AAs may suggest the origins of AAs from bacteria and marine phytoplankton. The ratios of D-form to L-form (D/L ratio) may indicate the input of biomass burning to atmospheric aerosols (Barbaro et al., 2020; Zangrando et al., 2016) as well as the degree of microbial degradation in atmospheric aerosols (Barbaro et al., 2015, 2020). The input from these sources will increase the D/L value of the corresponding AA.

AA enantiomers have been detected in atmospheric aerosols in the urban, marine and polar environment (Barbaro et al., 2019, 2020; Feltracco et al., 2019; Wedyan and Preston, 2008; Zangrando et al., 2016). D-AAs in aerosols from the Atlantic (marine) (Wedyan and Preston, 2008), Arctic (polar) (Feltracco et al., 2019), Alps (high altitude background site) (Barbaro et al., 2020), Venice (urban) (Barbaro et al., 2019), Serbia Belgrade (urban) (Zangrando et al., 2016) account for about 27%, 20%, 4.3%, 3% and 1% of the total AAs, respectively. D/L ratios of AAs in aerosol samples are usually used to investigate their sources and atmospheric processes. For example, the increase of D/L-Ala ratio in aerosols was found during biomass burning period. In a study in Belgrade (Serbia), the values were reported to be 0.88 and 0.23 during biomass burning and non-biomass burning periods, respectively. In Alpine aerosols, D/L-Ala was in the range of 0.7-1.7 in spring under the influence of biomass burning which was higher than that in summer (0.4-0.6).

The detection of AA enantiomers in aerosols is still a challenge due to their low abundances (especially D-AAs) and the influence of complex matrix effects (MEs) (Gorelsk et al., 1992). Water-soluble compounds in ambient samples are co-extracted with AAs, such as amino compounds, sugars, humic acids and ions. Amino compounds with similar chemical structures and properties may be involved in the process of derivatization and high concentrations of sugar may also affect the pH of the derivatization reaction of AAs (Wang et al., 2014). These may interfere the performance of the qualitative and quantitative analysis of AAs. High performance liquid chromatography (HPLC) is usually used for aerosol chiral AAs detection. Tandem mass spectrometry (MS/MS), ultra-violet detector (UVD) and fluorescence detectors (FLD) are the detectors reported by previous studies (Li et al., 2022; Song et al., 2017; Wang et al., 2019; Wedyan and Preston, 2008). Fluorescence detection is sensitive for the analysis of AAs. Before detection, derivatization is necessary to introduce chromophores for detection. For aerosol samples, the other critical step is to remove the complex MEs caused by the coexistence of aerosol components such as ions and carbonaceous fractions. Although HPLC-FLD analysis is one of the conventional separation methods for AAs, little is known about the causes and removals of ME when analyzing AAs in atmospheric aerosol.

In this study, we present a method for analyzing AA enantiomers in atmospheric aerosol samples. The MEs of coexistent aerosol components under different pollution conditions were investigated. Accordingly, the method was optimized to remove MEs, and to improve the separation and recovery of AAs. We further applied the method to determine AA enantiomers in real aerosol samples in urban environments with and without severe pollution. This work provides a useful method for the quantification of AA enantiomers in ambient aerosol samples which can help to obtain enantiomeric information of AAs for an in-depth understanding of the sources and atmospheric behaviors and impacts of aerosol proteinaceous matter in the atmosphere.

1. Experimental

1.1. *Sampling*

A total of 17 atmospheric aerosol samples from field campaigns were used in this study. All samples were collected on quartz filters which were pre-heated at 450°C and stored at −20°C in darkness before analysis. A high-volume air sampler (Tisch, US) was operated for sampling at a flow rate of 1.0 m^3/min. All samples were collected on the pre-baked quartz fibre filters (20 × 25 cm, Pall).

Eleven samples, including 4 marine aerosol total suspended particle (TSP) samples and 7 urban fine particulate matter ($PM_{2.5}$) samples, were used for method development. Four marine TSP samples were collected on in the ship cruising campaigns over the South China Sea in 2015 and 2016. The sampling duration was from 21 to 23 hr. Seven urban aerosol samples ($PM_{2.5}$) were collected in the campus of Tianjin University (TU) in Tianjin, China (117.17°N, 39.11°E) in 2016 and in Guangdong Environmental Monitoring Center (23.11°N, 113.33°E) in 2018. Each urban sample has a sampling duration of 12 hr.

Six urban $PM_{2.5}$ samples were also collected at TU during a pollution episode in winter of 2021. These samples were used

in this work to demonstrate the performance of method application for AA enantiomers measurements in ambient aerosol under pollution conditions.

1.2. Analysis of AA enantiomers in aerosol samples

1.2.1. Extraction of AAs

A part of each filter sample (equivalent to ~100 m^3 of air) was ultrasonically extracted twice for 30 min in an ice bath with 11 mL and 7 mL of sterile water (Barbaro et al., 2019; Matos et al., 2016; Samy et al., 2011; Zhang and Anastasio, 2003). The sterile water is prepared by ultrapure water after autoclaving (121°C, 30 min). Both extracts obtained from the extractions were put together and filtered through a syringe filter (0.45 μm cellulose acetate membrane, Jinlong, China). The filtered extracts were lyophilized and then were redissolved into 1 mL of sterile water for further analysis. After subsequent solid phase extraction treatment, the sample was stored in HCl (pH = 1) for analysis. Prior to HPLC analysis, L-homoarginine (L-hArg) was added as an internal standard (IS).

1.2.2. Pretreatment and purification of AAs

The solid phase extraction (SPE) columns were filled with 1.5 mL Dowex 50W × 8 H^+ (200-400 mesh) cationic resin. The resin (Dowex 50W × 8 H^+, 200-400 mesh) was filled in the tubes to prepare SPE columns. During the pretreatment, we used autoclaved (121°C, 30 min) ultrapure water (18.2 MΩ·cm) to prevent possible contamination of organic components and microbes. After conditioning of 5 mL HCl (2 mol/L), Dowex SPE columns were washed with sterile water till being neutralized. For purification, 0.5 mL of the sample was diluted with 0.5 mL of 0.2 mol/L HCl and then loaded into a Dowex SPE column. Sterile water was then used to rinse the column till being neutralized again. 5 mL of 4 mol/L ammonia in methanol was used to elute AAs enriched in the column. The collected effluent was further blown by N_2 (45°C) to dryness and the residue was redissolved in 0.5 mL HCl solution (0.1 mol/L) for HPLC-FLD analysis.

1.2.3. AA enantiomers analysis by HPLC-FLD

The analysis of AA enantiomers was performed using an HPLC-FLD system (1260, Agilent, Germany) with pre-column derivatization of o-phthaldialdehyde (OPA) and N-isobutyryl-L-cysteine (IBLC) (260 mmol/L and 170 mmol/L in 1 mol/L potassium borate buffer, pH = 10.4). The reaction of OPA derivatization for AAs is shown in Fig. 1. AA standards (purity ≥ 98%) including 24 AAs were listed in Table 1. L-hArg was selected as an IS. The method of IS correction is described in Appendix A. The standards were diluted in 0.1 mol/L HCl as standard stock solutions for further preparation of mix standard solution.

AAs were separated by a C18 column (Hypersil BDS C18, 250 × 4 mm, 5 μm) with a guard column (10 × 4 mm, 5 μm) using gradient elution (Kaufman and Manley, 1998; Wedyan and Preston, 2008). The mobile phase A was 23 mmol/L sodium acetate adjusted to pH 6.00 ± 0.02 with 10% acetic acids; mobile phase B was 100% methanol; mobile phase C was 100% acetonitrile; and mobile phase D was auto-claved ultrapure water. The gradient procedure is listed in Table S1. The flow-rate was 1.0 mL/min.

After analysis, the peak areas of AAs were corrected by the area of IS (L-hArg). The linear calibration curves based on corrected peak areas were established for quantification. The linearity of the calibration curve, instrument detection limits and resolutions of AAs were calculated to validate the analytical method.

1.3. Analyses of other chemical components

Water soluble ions (WSI), including chloride (Cl^-), nitrate (NO_3^-), sulfate (SO_4^{2-}), sodium (Na^+), ammonium (NH_4^+), potassium (K^+), calcium (Ca^{2+}), and magnesium (Mg^{2+}), were analyzed by ion chromatography (IC, ICS-600, Thermo, China). Organic carbon (OC) and elemental carbon (EC) were analyzed by a carbon analyzer using protocol of thermal optical transmission (TOT). The concentrations of organic carbon, elemental carbon and water-soluble ions in these samples are shown in Appendix A Table S2.

2. Results and discussion

2.1. Method application in ambient aerosol samples and matrix effects

The separation and detection of AA enantiomers were achieved by our method using HPLC-FLD. Fig. 2 shows the chromatogram of the analysis of 24 AAs standards (60 μmol/L) and L-hArg (IS) (36 μmol/L). They are completely separated and eluted out within 75 min. The instrument detection limit (IDL), instrument quantification limit (IDQ) and resolution were summarized in Table 1. The correlation coefficients (R^2) of calibration linearity were ≥0.99 for all 24 AAs. The IDL was 0.003-0.184 μmol/L and the range of IDQ was 0.009-0.225 μmol/L. The variable coefficient (CV) of peak area was used to evaluate the stability of derivatization. The CV value of L-hArg in AA standard series solutions was <10%. The resolutions of chromatographic separation of AAs were evaluated by a 2 μmol/L mixed standard solution. The details of resolution calculation is shown in Appendix A. It shows good resolutions (>1.5) for the separation of all AAs using this method (see Table 1).

The method was applied to analyze AA enantiomers in real aerosol samples. The influence of MEs was observed in the chromatograms including the suppression of fluorescence response, unknown peaks of co-eluting compounds and baseline drift. The ME value is defined as the ratio of peak area in sample matrix over peak area of standard. When the ratio is lower than 1, a suppression of signal caused by sample matrix is suggested. Based on the results of 4 marine aerosol samples and 7 urban samples for method development, we found that the ME values of less pollution and highly pollution samples are 0.72 and 0.31, respectively, when the peak area of 1 μmol/L L-hArg ($A_{L\text{-}hArg}$) was investigated (the peak areas are shown in Appendix A Fig S1). It clearly suggests that real aerosol sample matrix suppressed the AA signals.

Higher EC level presents more pollution feature of atmospheric aerosols. In this study, samples with EC concentration less than 1 μg/m^3 are regarded as less polluted samples while highly pollution samples are those with EC level higher than

Table 1 – Calibration linearity (R^2), instrument detection limit (IDL), instrument quantification limit (IDQ), method detection limit (MDL), quantification limit (MDQ) and resolution (R) of amino acid analysis using HPLC-FLD.

No.	Amino acid			IDL	IDQ	MDL	MDQ	Resolution	R^2
		acronym	MW (g/mol)	(μmol/L)	(μmol/L)	(μmol/L)	(μmol/L)	(R)	
1	L-aspartic acid	L-Asp	133.1	0.004	0.015	0.158	0.171	1.8	1.00
2	D-aspartic acid	D-Asp	133.1	0.017	0.057	0.134	0.207	24.8	0.99
3	L-glutamic acid	L-Glu	147.13	0.02	0.067	0.033	0.09	7.7	1.00
4	L-asparagine	L-Asn	132.12	0.01	0.033	0.061	0.187	8.7	1.00
5	L-serine	L-Ser	105.09	0.03	0.101	0.018	0.049	7.5	1.00
6	D-serine	D-Ser	105.09	0.001	0.005	0.043	0.145	7.2	0.99
7	L-glutamine	L-Gln	146.14	0.009	0.031	0.102	0.325	11.1	1.00
8	L-threonine	L-Thr	119.12	0.006	0.019	0.055	0.183	3.8	1.00
9	L-histidine	L-His	209.63	0.002	0.006	0.304	0.374	1.7	0.99
10	Glycine	Gly	75.07	0.016	0.055	0.202	0.324	15.4	1.00
11	L-arginine	L-Arg	210.66	0.033	0.11	0.218	0.257	3.9	1.00
12	L-alanine	L-Ala	89.09	0.033	0.11	0.076	0.254	7.5	0.99
13	D-alanine	D-Ala	89.09	0.161	0.225	0.213	0.418	9.2	0.99
14	L-tyrosine	L-Tyr	181.19	0.032	0.106	0.078	0.113	30.6	1.00
15	L-valine	L-Val	117.15	0.055	0.084	0.133	0.261	3.3	1.00
16	L-methionine	L-Met	149.21	0.054	0.067	0.044	0.146	7.4	1.00
17	L-tryptophan	L-Trp	204.23	0.184	0.211	0.226	0.37	4.1	1.00
18	D-methionine	D-Met	149.21	0.015	0.017	0.141	0.375	4.3	1.00
19	D-valine	D-Val	117.15	0.03	0.099	0.295	0.393	5.2	0.99
20	L-phenylalanine	L-Phe	165.19	0.071	0.088	0.083	0.275	2.2	1.00
21	L-isoleucine	L-Ile	131.17	0.035	0.118	0.083	0.277	16.2	1.00
22	L-leucine	L-Leu	131.17	0.029	0.097	0.098	0.223	2.8	1.00
23	D-isoleucine	D-Ile	131.17	0.029	0.098	0.018	0.061	8.4	1.00
24	D-leucine	D-Leu	131.17	0.003	0.009	0.101	0.337	8.4	1.00

4 μg/m^3. The stronger MEs were observed in those samples collected from highly pollution periods. We observed that the peaks of unknown compounds were co-eluted together with L-hArg and other AA peaks (Appendix A Fig. S1c). Baseline drift was frequently observed during the analysis of aerosol samples especially in those samples collected from the pollution periods.

Coexistent aerosol components such as organic species are the possible causes of MEs for AA analysis. More importantly, how to remove MEs in real sample matrix is critical for the improvement of method performance and the application in environmental research. Organic matter was reported as one of the major components in atmospheric aerosols (Tian et al., 2014; Wang et al., 2017). The MEs caused by organic matter were investigated in this study. We found that ammonium ion also cause interferences. The influence of organic matter was investigated using OC as a proxy while MEs caused by major water-soluble ions were also studied. We observed that the inhibition effect on AA fluorescence signals increased with the increase of OC concentration in aerosol samples. The ME caused by organic matter is exhibited by the plot between OC and ME value with a significant negative logarithmic correlation ($r^2 = 0.85$, Fig. 3a). It indicates that the decrease of fluorescence response of AAs is related to the presence of organic matter (proxied by OC) in aerosol samples. A possible reason is that aerosol organic matters is capable of absorbing the excitation or emission of fluorescence from derivatized AAs (MacDonald et al., 1997). The other reason could be due to the presence of some oxidation components in aerosols (Chen et al., 2018; Liu et al., 2021) which may reduce the efficiency of derivatization. Previous studies have pointed out that OPA is easily degraded by oxidation leading to an incomplete derivatization (Dai et al., 2014).

Among the peaks of co-eluting compounds, a wide peak (P_w) appears during the retention time from 50 to 60 min in the analysis of real aerosol samples, which interferes with the qualitative and quantitative determination of L-Met, L-Trp and D-Val (Appendix A Fig. S2a). A similar phenomenon was also observed in a previous study of AA analysis by the derivatization of OPA (Fitznar et al., 1999).

The derivatization of AAs is accomplished by their functional group of $-NH_2$ reacting with derivatization agents to form diastereomers having fluorophore which can be detected by FLD (Hess, 2019). We found that the interference of NH_4^+ is related to this mentioned broad peak. A solution of 0.01% NH_4^+ was analyzed using the same method and a similar peak was observed in the same retention time window (Appendix A Fig. S2a). A series of NH_4^+ concentrations in aerosol were measured to establish the correlation between NH_4^+ concentrations and the peak ratios of P_w peak area corrected by IS ($r^2 = 0.86$, Fig. 3b), confirming the interference of NH_4^+.

2.2. *Removal of matrix effects of coexistent aerosol components*

The Dowex 50W × 8 H^+ (200 - 400 mesh) resin has been applied in several studies to AA analysis in plant leaves, honey, rainwater and soil samples (Patzold and Brueckner, 2006;

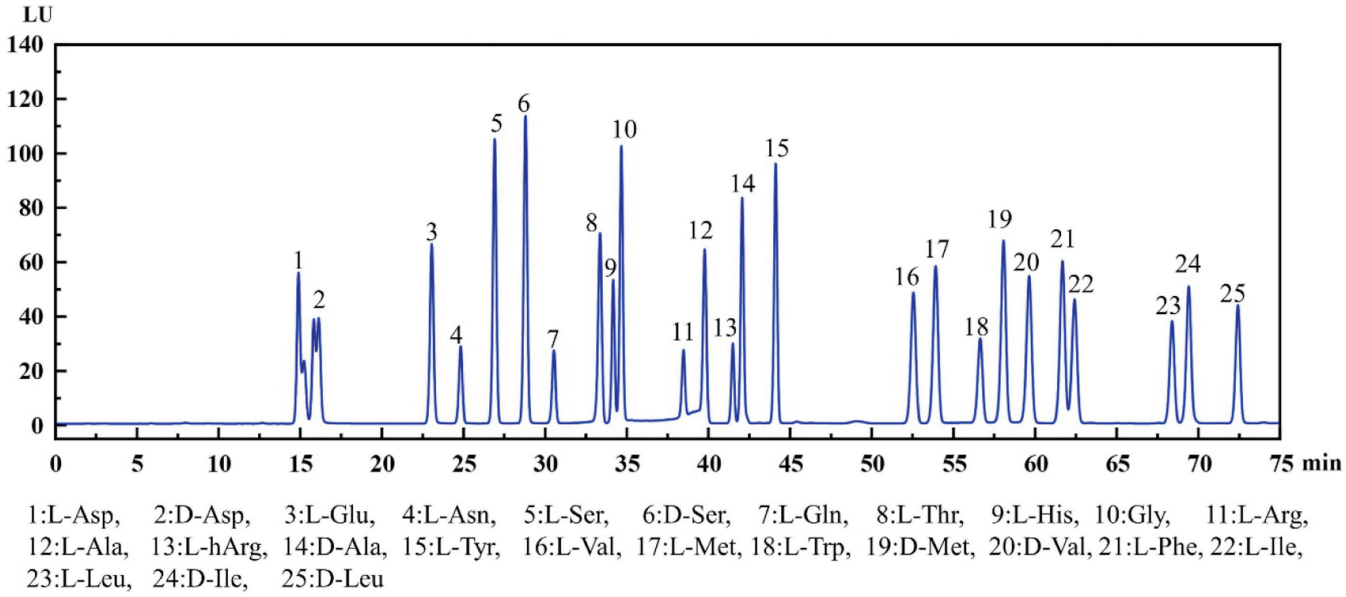

Fig. 2 – Chromatogram of amino acid analysis by HPLC-FLD with precolumn derivatization. The concentrations of amino acids are all 60 μmol/L. L-hArg is internal standard. The concentration of internal standard is 36 μmol/L.

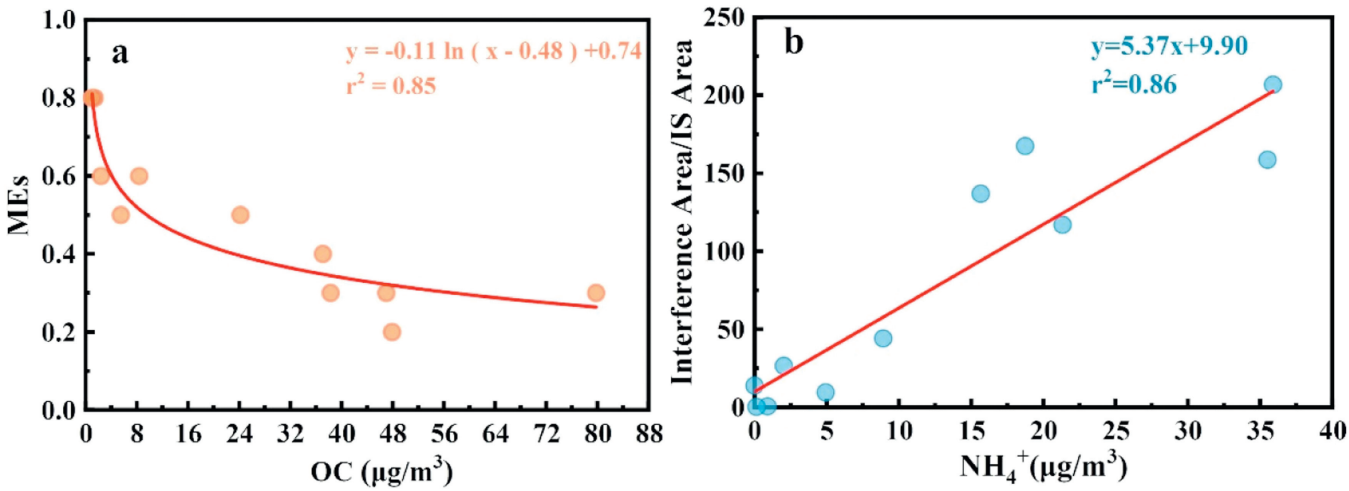

Fig. 3 – Matrix effects (MEs) of organic matter and ammonium ions on amino acidanalysis. (a) logarithmic relationship between ME value and organic carbon concentration in ambient aerosol samples; (b) linear relationship between the concentration of NH_4^+ and the areas of a broad peak in the retention time window of 50-60 min in standard solution.

Simeone et al., 2018; Xu and Xiao, 2017; Xu et al., 2020) showing its capability in ME removal. In order to remove MEs, SPE column loading with Dowex 50W × 8 H^+ (200 - 400 mesh) cationic resin was used in this study. After purification by Dowex SPE, most of the impurity peaks such as those co-eluting with Gly, L-hArg, L-Val, D-Val and D-Leu were removed, except the broad peak appearing in 50 - 60 min (Appendix A Fig. S2b). The ME may be due to the coexistent NH_4^+ in atmospheric aerosols. NH_4^+ may also come from the remain of methanol ammonia in the purification process. Therefore, when the extract was concentrated to 50 μL by N_2 blowing at 45°C, NaOH solution (1%) was used to adjust the extract to a highly alkaline environment (pH = 14) which is favorable for the volatilization of NH_3. The sample was re-dissolved in HCl to obtain a solution at a pH of 1 - 3, in consistent with that in standard solution. As shown in Appendix A Fig. S2b, the interference peak within 50-60 min was successfully eliminated by adding 1% NaOH (denoted as pretreatment of Dowex SPE-1% NaOH).

After pretreatment, the ME value for $A_{L\text{-}hArg}$ in real aerosol sample reaches 0.89, showing that the suppression of response has been solved (Appendix A Fig. S1). The baseline drift in chromatograms has also been greatly improved after pretreatment (see the baselines before and after pretreatment in real sample analysis in Appendix A Fig. S3). The baseline drifts are -30.04 LU/hr and 0.09 LU/hr before and after the pretreatment. The results suggest that the pretreatment of Dowex SPE-1% NaOH can effectively remove MEs in real sample analysis.

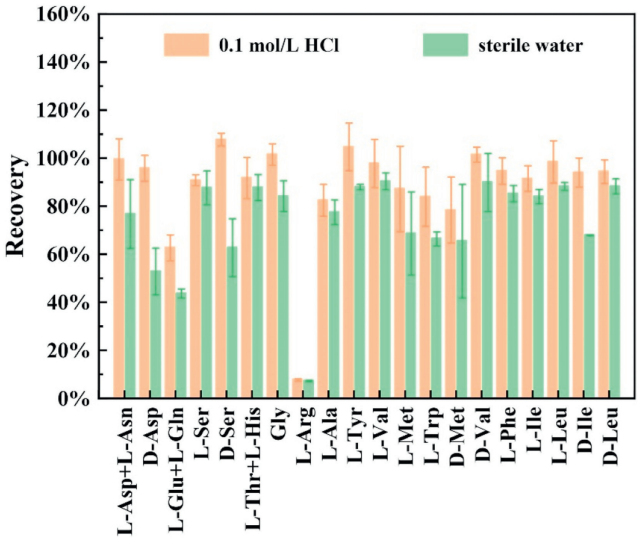

Fig. 4 – Recoveries of amino acids in solid phase extraction process using 0.1 mol/L HCl and sterile water.

2.3. *Improvement of AA enantiomers measurement and validation*

As mentioned above, pretreatment of Dowex SPE-1% NaOH removes the MEs of coexistent components in aerosol samples. However, we noticed that the recoveries of some AAs (such as L-Asp, D-Asp and D-Leu), which are important indicators to reveal the sources and atmospheric chemical processes of bioaerosols, decreased greatly in the extraction and pretreatment processes. Further measures should be implemented to improve the recoveries of AAs.

The isolation mechanism of AAs by cation exchange SPE includes ion binding and hydrophobic interaction (Gamon et al., 2020), and therefore, the efficiency of AA isolation by SPE depends on the charge, polarity, and size of the side chain groups of the AAs. The Dowex SPE is activated by 5 mL of 2 mol/L HCl, and as a result, the resin bonded with benzene sulfonic acid is negatively charged. The AAs could only be captured by the SPE column when they exist as cations in the extracted solution. For this purpose, the pH value of the extracted solution was adjusted to a value lower than the isoelectric points (pIs) of all the target AAs (Spanik et al., 2007), which is 2.27 (pI of Asp).

In our previous study, sterilized water was used as the media for aerosol extraction (Li et al., 2022; Song et al., 2017; Wang et al., 2019). We compared the recoveries of the target AAs in sterile water and 0.1 mol/L HCl and found that the recoveries in 0.1 mol/L HCl were 3%-45% higher than those in sterile water (Fig. 4), suggesting that 0.1 mol/L HCl is suitable for the treatment process. After lyophilized, the extracts were redissolved in 1 mL of sterile water. Before SPE procedure, we diluted the sample 1:1 with 0.2 mol/L HCl. Dilution of the sample with acid did not affect the recoveries (Appendix A Fig. S4). The recoveries of Asp and Asn were reported in the forms of L-Asp + L-Asn and L-Glu and L-Gln because Gln and Asn completely conversed to Glu and Asp in the presence of NaOH. Among the AAs, the recovery of D-Asp in sterile water was about 50% while it reached 95% in 0.1 mol/L HCl. However, the recovery of Arg was lower than 10%, which is possibly due to its high pI (10.76), leading to the tight binding of Arg to the SPE column.

Considering the competitive adsorption of AAs by SPE column, we prepared an AA solution in 0.1 mol/L HCl, whose concentrations of AAs are similar to those in urban aerosol extract (Appendix A Table S3), to obtain the recoveries after pH optimization. Among the target AAs, recoveries of 17 AAs were above 77%, except those of L-Glu + L-Gln and D-Val (Group II) (64% and 60%, respectively, Appendix A Table S3). In order to validate the analytical methods on environmental samples, the recovery should be optimized in a certain range considering the loading of analytes in samples. However, in real sample analysis, the recovery could still be in a relatively lower level when analytes are co-existed with complicated matrix. Our results show that the recoveries of SPE treatment should meet the requirement of AA analysis for most of the aerosol samples after pH optimization.

After Dowex SPE-1% NaOH pretreatment and pH optimization, the analytical limits of detection (MDL, 3 sec method) and quantification (MDQ, 10 sec method) of the AA analysis method for aerosol samples are 0.018-0.304 μmol/L and 0.049-0.418 μmol/L, respectively (n = 3). Similar recoveries were observed for blank filter samples (n=3) and aerosol filter samples (n = 3) spiked with 200 μL of 30 μmol/L AA standards solution. As presented in Table 2, the detected AAs are classified into three groups. The recoveries of 13 AAs (Group I) in the spiked aerosol samples were all higher than 75%, and those of 5 AAs in Group II were in the range of 50%-75%. For the 4 AAs in Group III, their recoveries were lower than 50%. L-Arg, L-Met and D-Met are expected to be captured by the SPE column and L-Trp should be lost in the extraction process. The recoveries of those enantiomers in Group I meet the requirements (75%-125%) for the detection of analytes with content <0.1% in the sample. For the enantiomers in Group II, improvements are necessary to optimize the recoveries in the future. For those in Group III, it should be very careful to apply the analysis and should impose further concerns in their characterization on real samples.

2.4. *Measurement of AA enantiomers in urban aerosols under different pollution conditions*

We then applied the optimized method to analyze AAs in aerosol samples collected in Tianjin, China, including samples collected in pollution and non-pollution periods. The total free amino acid concentrations (TFAAs) in aerosol samples were 126.7 ± 37.8 and 23.7 ± 19.7 ng/m^3 during the pollution and non-pollution period, respectively. The average concentration of TFAAs in the pollution episode is comparable to those observed at urban sites in Tokyo, Japan and Rome, Italy (Abe et al., 2016; Di Filippo et al., 2014). The concentration of TFAAs in the non-pollution period was comparable to those observed in Jeju Island, South Korea (rural site) and Nanchang (forest site), China (Yang et al., 2004; Zhu et al., 2020). A total of 19 AAs were detected in the samples. The concentration and composition of AAs are shown in Fig. 5a and those of D-AAs are shown in Fig. 5b. Although the D-AAs are in low

Table 2 – Recoveries and precisions of amino acids (AAs). Whole process recovery and precision of spiked standard mixed solution of AAs on blank quartz filter and $PM_{2.5}$ filter.

Group	No.	Amino acid (AAs)	spiked sample on blank filter (30 μmol/L AAs)		spiked sample on $PM_{2.5}$ filter (30 μmol/L AAs)	
			Recovery	RSD ($n = 3$)	Recovery	RSD ($n = 3$)
I	1	L-Asp+L-Asn	80%	3%	102%	4%
	2	L-Ser	98%	10%	103%	3%
	3	Gly	108%	6%	106%	5%
	4	L-Ala	63%	9%	102%	3%
	5	D-Ala	85%	5%	84%	2%
	6	D-Asp	78%	8%	101%	6%
	7	D-Ser	76%	2%	105%	4%
	8	L-Thr	73%	9%	104%	2%
	9	L-Val	80%	4%	96%	9%
	10	L-Ile	75%	5%	80%	6%
	11	L-Phe	64%	10%	86%	4%
	12	D-Ile	71%	3%	79%	2%
	13	L-Tyr	64%	8%	79%	2%
II	14	L-His	105%	12%	72%	5%
	15	D-Leu	72%	2%	71%	1%
	16	L-Leu	81%	2%	71%	4%
	17	L-Glu+L-Gln	53%	7%	67%	2%
	18	D-Val	76%	3%	67%	4%
III	19	L-Arg	15%	12%	11%	19%
	20	L-Met	34%	18%	14%	5%
	21	L-Trp	15%	14%	36%	7%
	22	D-Met	21%	43%	12%	7%

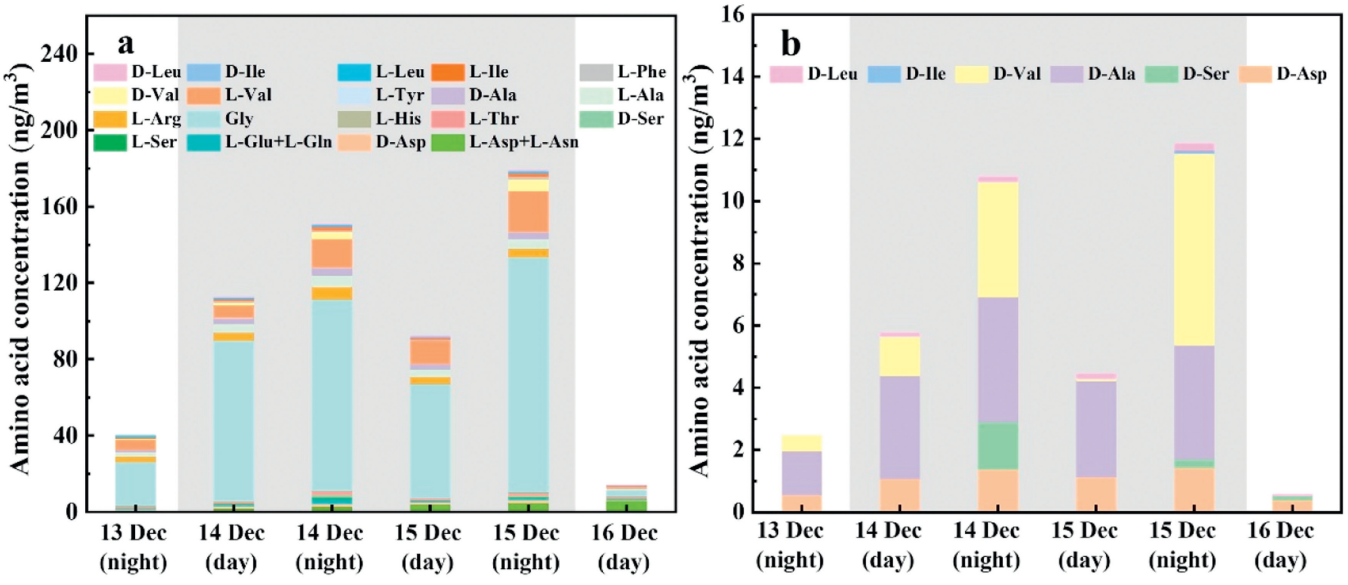

Fig. 5 – Concentrations of amino acid enantiomers in atmospheric aerosol collected in Tianjin, China in a pollution episode in December 2021. (a) all enantiomers; (b) D-enantiomers. The shadows present the pollution episode.

abundance, 6 D-AAs were determined among the AAs (Fig. 5), i.e., D-Val, D-Ala, D-Ser, D-Leu, D-Ile and D-Asp. Their concentrations were 2.34 ng/m^3, 3.10 ng/m^3, 0.64 ng/m^3, 0.14 ng/m^3, 0.10 ng/m^3 and 0.99 ng/m^3, respectively. D-AAs averagely accounted for 6% of the TFAAs, higher than that of 3% in Venice (Barbaro et al., 2019), indicating that higher bacterial contribution was expectedto atmospheric aerosols in Tianjin. Gly, L-Val, L-Ala and D-Ala were the dominant AAs in both pollutionand non-pollution periods. The high percentage of Gly was frequently reported in previous studies (Di Filippo et al., 2014; Feltracco et al., 2019; Zhu et al., 2020), which is related to the high stability and low photochemical reactivity of Gly. The contribution of Gly increased from 55% in the non-pollution period to 72% in the pollution period while the abundances

of L-Ala and D-Ala were reduced from 6% and 6% to 4% and 3%, respectively. The relative abundances of Gly (55%) and D-Ala (6%) in the non-pollution period are close to those reported by a previous study in Svalbard Islands in the Arctic (Feltracco et al., 2019), which were less disturbed by human activities.

The D/L ratio can be used as an indicator to reveal the sources of aerosols. Previous studies found that biomass combustion might increase the D/L-Ala value (Barbaro et al., 2020; Feltracco et al., 2019; Zangrando et al., 2016). In this study, D/L-Ala, D/L-Ser and D/L-Val in the pollution period were higher than those in the non-pollution period, suggesting that samples in the pollution period were more affected by biomass burning (Broek et al., 2019). At the same time, the D/L of AAs can indicate the degree of microbial degradation (Tremblay and Benner, 2006). Higher D/L values of AAs during the pollution period point to a higher degree of microbial degradation. Notably, the presence of D-Ile and D-Leu indicate a potential source of marine phytoplankton. In this study, the D/L-Leu in non-pollution period was higher than in pollution period, indicating the relatively higher contribution of marine source in the non-pollution period.

3. Conclusions

In this study, we demonstrate an effective method using HPLC-FLD for the analysis of AA enantiomers in atmospheric aerosol samples. Our results reveal that aerosol coexistent components can cause strong MEs for AA enantiomers analysis in atmospheric aerosols. Organic fractions and NH_4^+ are suggested as the major contributors to the observed MEs. An SPE with Dowex resin (50W $\times$ 8 H^+, 200 - 400 mesh) followed by a NaOH adjustment was applied to remove the two fractions. After Dowex SPE-NaOH pretreatment, MEs, including AA fluorescence response suppression, unknown peaks from co-eluting compounds, and baseline drift, have been removed for improved performance in qualitative and quantitative analysis of AA enantiomers.Besides, recoveries of AAs were improved after pH adjustment of the sample extract. The method allows the acquirement of satisfactory enantio-resolution of 6 D-AAs and quantification of 12 AAs (including 11 L-AAs and Gly) in one analysis. In order to understand the performance of the method, we applied this method to analyze the urban aerosol samples collected in Tianjin during a pollution episode with complex organic and ionic matrix. The abundances and D/L ratios of AAs were comparable to those from previous studies. AA enantiomers were successfully detected and quantified in all samples. The D/L ratios suggest that the pollution event in Tianjin was significantly influenced by biomass combustion. In general, this optimized HPLC-FLD method is a promising tool for AA enantiomers detection in atmospheric aerosol and can be applied in atmospheric studies to improve the understanding of AA enantiomers in environment.

Declaration of Competing Interest

The authors declare that they have no known competing financial interests or personal relationships that could have appeared to influence the work reported in this article.

Acknowledgments

This work was supported by the Natural Science Foundation of China (No. 41975156).

Appendix A Supplementay data

Supplementary material associated with this article can be found in the online version at doi:10.1016/j.jes.2023.02.048.

References

Abe, R.Y., Akutsu, Y., Kagemoto, H., 2016. Protein amino acids as markers for biological sources in urban aerosols. Environ. Chem. Lett. 14 (1), 155–161.

Barbaro, E., Feltracco, M., Cesari, D., Padoan, S., Zangrando, R., Contini, D., et al., 2019. Characterization of the water soluble fraction in ultrafine, fine, and coarse atmospheric aerosol. Sci. Total Environ. 658, 1423–1439.

Barbaro, E., Morabito, E., Gregoris, E., Feltracco, M., Gabrieli, J., Varde, M., et al., 2020. Col Margherita observatory: a background site in the Eastern Italian Alps for investigating the chemical composition of atmospheric aerosols. Atmos. Environ. 221 (1), 117071.

Barbaro, E., Zangrando, R., Vecchiato, M., Piazza, R., Cairns, W.R.L., Capodaglio, G., et al., 2015. Free amino acids in Antarctic aerosol: potential markers for the evolution and fate of marine aerosol. Atmos. Chem. Phys. 15 (10), 5457–5469.

Broek, T.A.B., Bour, A.L.B., Ianiri, H.L., Guilderson, T.P., McCarthy, M.D., 2019. Amino acid enantiomers in old and young dissolved organic matter: Implications for a microbial nitrogen pump. Geochim. Cosmochim. Acta 247, 207–219.

Chan, M.N., Choi, M.Y., Ng, N.L., Chan, C.K., 2005. Hygroscopicity of water-soluble organic compounds in atmospheric aerosols: amino acids and biomass burning derived organic species. Environ. Sci. Technol. 39 (6), 1555–1562.

Chen, Q., Sun, H., Wang, M., Mu, Z., Wang, Y., Li, Y., et al., 2018. Dominant fraction of EPFRs from nonsolvent-extractable organic matter in fine particulates over Xi'an. China. Environ. Sci. Technol. 52 (17), 9646–9655.

Dai, Z., Wu, Z., Jia, S., Wu, G., 2014. Analysis of amino acid composition in proteins of animal tissues and foods as pre-column o-phthaldialdehyde derivatives by HPLC with fluorescence detection. J. Chromatogr. B Analyt. Technol. Biomed. Life. Sci. 964, 116–127.

Di Filippo, P., Pomata, D., Riccardi, C., Buiarelli, F., Gallo, V., Quaranta, A., 2014. Free and combined amino acids in size-segregated atmospheric aerosol samples. Atmos. Environ. 98, 179–189.

Dittmar, T., Fitznar, H.P., Kattner, G., 2001. Origin and biogeochemical cycling of organic nitrogen in the eastern Arctic Ocean as evident from D- and L-amino acids. Geochim. Cosmochim. Acta 65 (22), 4103–4114.

Feltracco, M., Barbaro, E., Kirchgeorg, T., Spolaor, A., Turetta, C., Zangrando, R., et al., 2019. Free and combined L- and D-amino acids in Arctic aerosol. Chemosphere 220, 412–421.

Fitznar, H.P., Lobbes, J.M., Kattner, G., 1999. Determination of enantiomeric amino acids with high-performance liquid chromatography and pre-column derivatisation with o-phthaldialdehyde and N-isobutyrylcysteine in seawater and fossil samples (mollusks). J. Chromatogr. A 832 (1-2), 123–132.

Gamon, L.F., Guo, C.R., He, J.F., Hagglund, P., Hawkins, C.L., Davies, M.J., 2020. Absolute quantitative analysis of intact and oxidized amino acids by LC-MS without prior derivatization. Redox. Bio. 36, 101586.

Gorelsk, K., Galloway, J.N., Watterson, K., Keene, W.C., 1992. Water-soluble primary amine compounds in rural continental precipitation. Atmos. Environ. 26 (6), 1005–1018.
Hess, S., 2019. A universal HPLC-MS method to determine the stereochemistry of common and unusual amino acids. Methods Mol. Biol. 2030, 263–275.
Kaufman, D.S., Manley, W.F., 1998. A new procedure for determining DL amino acid ratios in fossils using reverse phase liquid chromatography. Quat. Sci. Rev. 17 (11), 987–1000.
Li, X., Zhang, Y., Shi, L., Kawamura, K., Kunwar, B., Takami, A., et al., 2022. Aerosol proteinaceous matter in coastal Okinawa, Japan: influence of long-range transport and photochemical degradation. Environ. Sci. Technol. 56 (8), 5256–5265.
Liu, X., Yang, L., Liu, G., Zheng, M., 2021. Formation of Environmentally persistent free radicals during thermochemical processes and their correlations with unintentional persistent organic pollutants. Environ. Sci. Technol. 55 (10), 6529–6541.
MacDonald, B.C., Lvin, S.J., Patterson, H., 1997. Correction of fluorescence inner filter effects and the partitioning of pyrene to dissolved organic carbon. Anal. Chim. Acta 338 (1-2), 155–162.
Matos, J.T.V., Duarte, R.M.B.O., Duarte, A.C., 2016. Challenges in the identification and characterization of free amino acids and proteinaceous compounds in atmospheric aerosols: a critical review. Trac-Quat. Sci. Rev. 75, 97–107.
McCarthy, M.D., Hedges, J.I., Benner, R., 1998. Major bacterial contribution to marine dissolved organic nitrogen. Science 281 (5374), 231–234.
Patzold, R., Brueckner, H., 2006. Gas chromatographic detection of D-amino acids in natural and thermally treated bee honeys and studies on the mechanism of their formation as result of the Maillard reaction. Eur. Food Res. Technol. 223 (3), 347–354.
Perez, M.T., Pausz, C., Herndl, G.J., 2003. Major shift in bacterioplankton utilization of enantiomeric amino acids between surface waters and the ocean's interior. Limnol. Oceanogr. 48 (2), 755–763.
Samy, S., Robinson, J., Hays, M.D., 2011. An advanced LC-MS (Q-TOF) technique for the detection of amino acids in atmospheric aerosols. Anal. Bioanal. Chem. 401 (10), 3103–3113.
Scalabrin, E., Zangrando, R., Barbaro, E., Kehrwald, N.M., Gabrieli, J., Barbante, C., et al., 2012. Amino acids in Arctic aerosols. Atmos. Chem. Phys. 12 (21), 10453–10463.
Simeone, G.D., Benesch, M., Glaser, B., 2018. Degradation products of polycondensed aromatic moieties (black carbon or pyrogenic carbon) in soil: Methodological improvements and comparison to contemporary black carbon concentrations. J. Plant Nutr. Soil Sci. 181 (5), 714–720.
Song, T., Wang, S., Zhang, Y., Song, J., Liu, F., Fu, P., et al., 2017. Proteins and amino acids in fine particulate matter in rural Guangzhou, Southern China: seasonal cycles, sources, and atmospheric processes. Environ. Sci. Technol. 51 (12), 6773–6781.
Spanik, I., Horvathova, G., Janacova, A., Krupcik, J., 2007. On the use of solid phase ion exchangers for isolation of amino acids from liquid samples and their enantioselective gas chromatographic analysis. J. Chromatogr. A 1150 (1-2), 145–154.
Szyrmer, W., Zawadzki, I., 1997. Biogenic and anthropogenic sources of ice-forming nuclei: a review. Bull. Am. Meteorol. Soc. 78 (2), 209–228.
Tian, S., Pan, Y., Liu, Z., Wen, T., Wang, Y., 2014. Size-resolved aerosol chemical analysis of extreme haze pollution events during early 2013 in urban Beijing. China. J. Hazard. Mater. 279, 452–460.
Tremblay, L., Benner, R., 2006. Microbial contributions to N-immobilization and organic matter preservation in decaying plant detritus. Geochim. Cosmochim. Acta 70 (1), 133–146.
Wang, Q., Jiang, N., Yin, S., Li, X., Yu, F., Guo, Y., et al., 2017. Carbonaceous species in $PM_{2.5}$ and PM_{10} in urban area of Zhengzhou in China: Seasonal variations and source apportionment. Atmos. Res. 191, 1–11.
Wang, S., Song, T.L., Shiraiwa, M., Song, J.W., Ren, H., Ren, L.J., et al., 2019. Occurrence of aerosol proteinaceous matter in urban Beijing: an investigation on composition, sources, and atmospheric processes during the "APEC Blue" period. Environ. Sci. Technol. 53 (13), 7380–7390.
Wang, Y.Q., Ye, D.Q., Zhu, B.Q., Wu, G.F., Duan, C.Q., 2014. Rapid HPLC analysis of amino acids and biogenic amines in wines during fermentation and evaluation of matrix effect. Food Chem. 163, 6–15.
Wedyan, M.A., Preston, M.R., 2008. The coupling of surface seawater organic nitrogen and the marine aerosol as inferred from enantiomer-specific amino acid analysis. Atmos. Environ. 42 (37), 8698–8705.
Xu, Y., Xiao, H., 2017. Concentrations and nitrogen isotope compositions of free amino acids in Pinus massoniana (Lamb.) needles of different ages as indicators of atmospheric nitrogen pollution. Atmos. Environ. 164, 348–359.
Xu, Y., Xiao, H.Y., Wu, D.S., Long, C.J., 2020. Abiotic and biological degradation of atmospheric proteinaceous matter can contribute significantly to dissolved amino acids in wet deposition. Environ. Sci. Technol. 54 (11), 6551–6561.
Yang, H., Xu, J.H., Wu, W.S., Wan, C.H., Yu, J.Z., 2004. Chemical characterization of water-soluble organic aerosols at Jeju Island collected during ACE-Asia. Environ. Chem. 1 (1), 13–17.
Zangrando, R., Barbaro, E., Kirchgeorg, T., Vecchiato, M., Scalabrin, E., Radaelli, M., et al., 2016. Five primary sources of organic aerosols in the urban atmosphere of Belgrade (Serbia). Sci. Total Environ. 571, 1441–1453.
Zhang, Q., Anastasio, C., 2003. Free and combined amino compounds in atmospheric fine particles ($PM_{2.5}$) and fog waters from Northern California. Atmos. Environ. 37 (16), 2247–2258.
Zhu, R.G., Xiao, H.Y., Zhu, Y.W., Wen, Z.Q., Fang, X.Z., Pan, Y.Y., 2020. Sources and transformation processes of proteinaceous matter and free amino acids in $PM_{2.5}$. J. Geophys. Res. Atmos. 125 (5), e2020JD032375.